RERTR 2008 — 30th INTERNATIONAL MEETING ON REDUCED ENRICHMENT FOR RESEARCH AND TEST REACTORS

October 5-9, 2008
Hamilton Crowne Plaza Hotel
Washington, D.C. USA

SWELLING OF U_3Si_2 DURING IRRADIATION

Yeon Soo Kim, G.L. Hofman, J. Rest
Argonne National Laboratory
9700 S Cass Avenue, Argonne, IL 60439

A.B. Robinson
Idaho National Laboratory
P.O. Box 1625, Idaho Falls, ID 83415-6188

Abstract

An irradiated U_3Si_2 dispersion fuel plate (U0R040) from the RERTR-8 test was metallographically examined. Large fission gas bubbles were observed. The fuel temperature was higher than for most of the previous silicide-fuel tests. The apparent causes for the high bubble growth are high fission density (5.2×10^{21} f/cm^3) and high fuel temperature (life-average 136°C). Analysis of PIE results of U0R040 and previous ANL test plates required modification of the existing athermal bubble growth model applicable to low temperature (below 110°C) for high temperature application (above 130°C). A more-detailed analysis was performed using a new fission gas bubble growth model developed at ANL to model the effect of the increased fuel temperature. Some of the results are reported in this paper. A threshold curve above which interconnected large bubbles form is proposed in terms of fuel temperature and fission density.

1. Introduction

Before the interest in developing U-Mo fuel prevailed, U_3Si_2 fuel received numerous tests both in-pile and out-of-pile. As a result, a considerable literature has been accumulated. U_3Si_2 is presently considered the best fuel qualified so far in terms of uranium loading and performance. In U_3Si_2/Al dispersion fuel, interaction layers grow slower than in U-Mo/Al dispersions. The interaction layers (ILs) in U_3Si_2/Al are free of porosity formation, in contrast to U-Mo/Al.

Fission gas bubbles in the unreacted fuel particles are generally small and stable except under extremely high burnup and/or high-temperature conditions. In the past, fission gas bubble growth and fuel swelling has been considered athermal in the relatively low (<110°C) temperature regime and dependent only on burnup.

Recently, potential applications of this fuel in high-power reactors rekindled an interest for additional tests [1-3]. The high-power reactor applications call for high heat fluxes (~260 W/cm^2), high burnups (~5×10^{21} f/cm^3), and high fuel temperatures (~140°C). In this paper, fission rates and densities include not only U-235 fissions but also those of U-238 atoms and of Pu atoms generated during irradiation. Although extensive data for the silicide fuel are available at ANL and in the literature, no data have been obtained at temperatures higher than 110°C combined with high burnups. Some previous tests were at high temperatures, but the burnups were low [4,5].

In the RERTR-8 test, devoted to U-Mo fuels, two U_3Si_2/Al dispersion fuel plates were included for normalization. The silicide fuel samples were irradiated under conditions similar to those for the U-Mo plates; these conditions were much more severe than those seen by most of the silicide fuels tested previously. The silicide plate irradiated at the higher power location has been metallographically examined. Metallography showed that the bubbles in some high-power regions of the plate are much larger than the maximum-size bubbles observed in prior tests. The large bubbles are distributed across all of the fuel particles seen in the optical micrographs. The maximum bubble size observed in the peak power region is ~40 μm, which the existing athermal bubble-growth model cannot reproduce. Unless a temperature effect is considered, the discrepancy cannot be resolved. In addition, some of the large bubbles have begun to interconnect. It should be noted that the condition for fuel plate failure by breakaway swelling is the interconnection of fission gas bubbles throughout a significant area of the fuel meat.

2. Irradiation test

Two U_3Si_2/Al dispersion fuel plates were included in the RERTR-8 test. The U-loading was 4.7 gU/cm^3 of meat. The plate irradiated at the higher-power location, C-6, in the test vehicle (U0R040) was metallographically examined. Plate U0R040 was irradiated for 104.7 effective full power days (EFPDs) with an average fission density of 4.6×10^{21} f/cm^3. The fuel enrichment was 74.9% U-235. The meat-average heat flux was 263 W/cm^2 at beginning of life (BOL) and decreased cycle-by-cycle to 177 W/cm^2 at end of life (EOL) [6].

Postirradiation gamma scans showed that substantial power peaks existed in the plate, not only transversely but also axially. The transverse power peaking occurs because the plate was loaded in the test vehicle with one side closer to the reactor core than the other side. The axial peaking is not as severe as the transverse peaking because the plate was irradiated in an axial location where the neutron flux is relatively flat. The magnitude of power peaking increases with enrichment. Axial power peaking is negligible for LEU plates whereas it is considerable for highly enriched fuel such as U0R040.

In Fig. 1(a), the dots schematically show the points where the plate thickness data were obtained. In this report, a thickness measurement point is written as (x,y) where x represents the transverse lines designated A - F and y represents the axial lines designated 1 - 3. The fission densities of U0R040 in the meat area, calculated from the gamma scan data and plate power data, are plotted in Fig. 1(b), where the thickness measurement points are also indicated.

A transverse section from the axial midplane of the meat, i.e., 2.5 mm below line D, was examined by optical metallography, as is the usual practice for RERTR test plates. However, as seen in the fission density map, the peak fission density occurs at the top corner of the plate near the measurement point (F,3), where the heat flux is estimated to be ~363 W/cm^2. Therefore, additional metallography was performed on a section cut along line 3 from the top of the meat to a point midway between (E,3) and (F,3).

3. Results

As shown in Fig. 2, postirradiation metallography of the transverse section of U0R040 at the axial midplane of the meat revealed smaller bubbles (~2 μm in diameter) on the cold side, i.e., near (D,1) and large fission gas bubbles (~20 μm in diameter) on the hot side, i.e., near (D,3). The bubble growth near (D,1) is similar to that observed in the previous low-temperature tests.

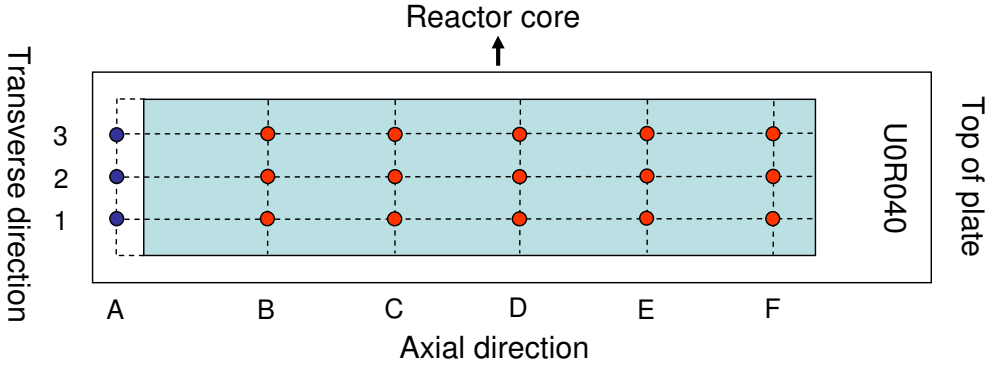

(a) Plate thickness measurement points. The meat axial midplane is located 2.5 mm below line D.

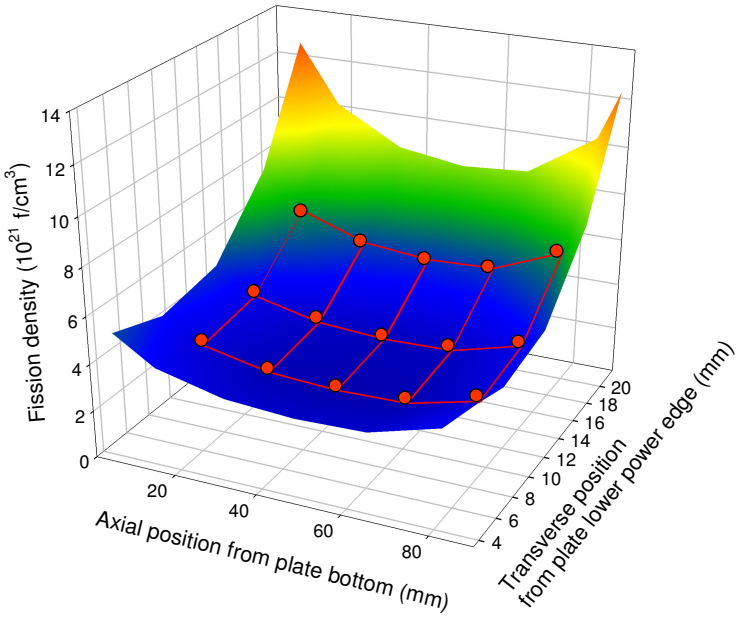

(b) Fission density map of U0R040 meat.

Fig. 1. Plate thickness measurement points and fission density map of U0R040. The red dots in (a) and (b) show the points where plate thicknesses were measured.

The large gas bubbles near (D,3) indicate unstable bubble growth that resulted in high fuel swelling. The growth of abnormally large bubbles is caused by interconnection of small bubbles that can result in fuel failure by pillowing. The bubble size measured at (F,3) is ~40 μm. The interaction between the fuel and matrix is so great that only a tiny bit of the Al matrix remains. Some of the large bubbles are starting to interconnect, which is a preliminary step for pillowing.

A lower magnification micrograph, not included here, shows that large bubbles are present throughout the fuel meat cross section, but some fuel particles generally have smaller bubbles than nearby particles. However, the extent of bubble growth is similar to that of U_3Si from previous tests, which is known to have faster bubble growth than U_3Si_2.

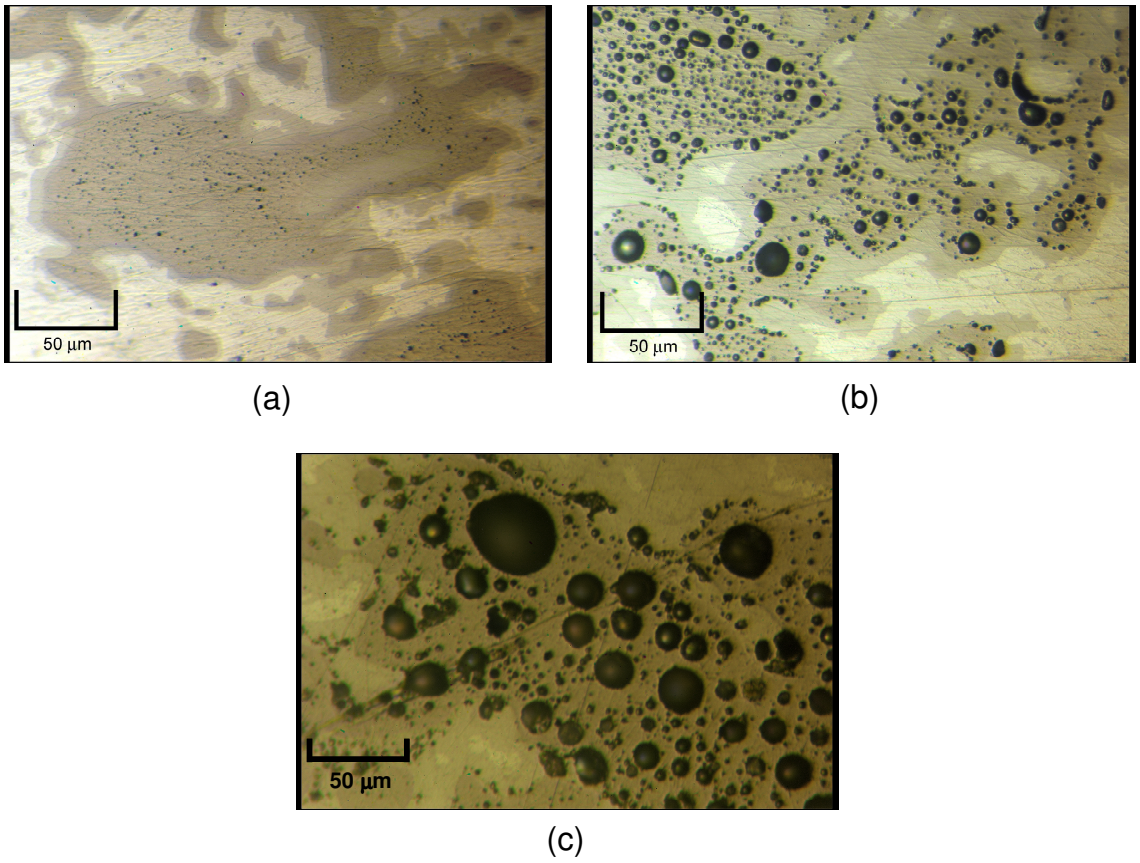

Fig. 2. Optical micrographs of U0R040 irradiated in ATR. (a) near (D,1) where T=106°C and FD=3.1 × 10^{21} f/cm^3; (b) near (D,3) where T=136°C and FD=5.2 × 10^{21} f/cm^3; (c) near (F,3) where T=160 °C and FD=6.5 × 10^{21} f/cm^3.

Fuel temperatures are calculated by using the IL growth correlation developed for U_3Si_2/Al dispersion fuel at ANL [5,7]:

$$Y = \left[A^{irr} \exp\left(-Q^{irr} / RT\right) \dot{f}^{0.5} t\right]^{0.5}, \quad (1)$$

where Y = interaction layer thickness (µm) $A^{irr} = 2.2\times10^{-8}$, $Q^{irr} = 9700$ cal/mol, R = universal gas constant (1.987 cal/K·mol), T = life-average fuel meat temperature (K), $\dot{f}$ = fission rate (fiss/cm^3·s), and t = irradiation time (s). For a test plate with known $\dot{f}$ and t, T can be calculated based on the measured IL thickness.

Table 1 Summary of irradiation data of U_3Si_2/Al

Test reactor (Sample ID)	Enrichment	Time EFPD	FR ♣ 10^{14} f/cm^3·s	FD ★ 10^{21} f/cm^3	T ♣ (°C)	IL (µm)	Bubble size (µm) †	Inter-connected bubbles	Data Source
BR-2 (1st test)	35			1.3	240		< 1	No	[1]
JMTR (88F-01)	19.8	108	1.8	1.7	200	10.0	2	No	[4]

ATR (R5-U6008J)	19.5	116	1.9	1.9	109	3.0	0.6	No	✧
ATR (R1-W002) *	19.5	94	2.6	2.1	65	1.0	0.4	No	✧
ORR (A100)	19.8	174	1.4	2.1	90	2.0	0.6	No	✧
HANARO (KOMO-3)⌖	19.5	206	1.4	2.5	142	6.0	3	No	[8]
ATR (R8-U0R040)C	74.9	105	3.4	3.1	106	3.1	2	No	♦
ATR (R2-W003)	19.5	232	1.8	3.6	65	2.0	0.6	No	✧
ORR (A99)	19.8	385	1.3	4.2	100	4.0	1	No	✧
FRJ-2 (Test 1-#10)	19.7	321	1.4	4.0	130	6.0	6	No	[9]
BR-2 (2nd test)	19.9	69	8.1	4.8	135	4.8	3	No	[2]
HFIR (HANS 3-10)	19.8	23	25.0	5.0	220	10.0	6	Yes	✧
ATR (R8-U0R040)H	74.9	105	5.7	5.2	136	5.6	20	No §	♦
NRU ⌖ (FL-050 center)	19.7	238	2.8	5.7	137	7.0	6	No	[10]
ATR (R8-U0R040)P	74.9	105	7.3	6.5	160	8.2	38	Yes	♦
ORR (A121)	92.6	130	8.4	9.4	100	3.2	3	No	✧
ORR (A122)	92.6	272	6.1	14.3	100	4.4	15	No	✧

♣ The fission rate and temperature are the life-averaged values. ★ Fission density is for fuel particles. † Diameter of maximum-size bubble; threshold size for an unstable bubble is tentatively set at 5 μm. ✧ Data obtained in previous ANL tests and reanalyzed in the present study. ♦ Data obtained in the present study. * R is an abbreviation of RERTR such that, for example, R1 means the RERTR-1 test. § Some bubbles show the initial stage of interconnection. ⌖ HANARO and NRU data are for rod-type fuel, all other data are for plate-type fuel. C = near (D,1), H = near (D,3), P = near (F,3) points in Fig. 1(a).

The results of the analysis of U0R040 data are given in Table 1. The test data available in the literature and by private communication, as well as previous ANL in-house data, are also included in the table. When the temperatures were not known, the life-average fission rate, measured IL thickness, and irradiation time were used in Eq. (1) to calculate the life-average fuel temperature. The JMTR [4] and HFIR [5] tests had nearly constant temperatures during the test, whereas all other tests had changing temperatures over the irradiation period. The temperatures of the JMTR and HFIR tests were confirmed by comparing with the calculated values using Eq. (1).

4. Discussion of postirradiation results

A plot of fuel temperature versus fission density for the previous tests and for the recent U0R040 test is shown in Fig. 3. The uncertainties in calculated temperatures are due mostly to errors involved in IL thickness measurements; the uncertainty in FD is small (less than 5%).

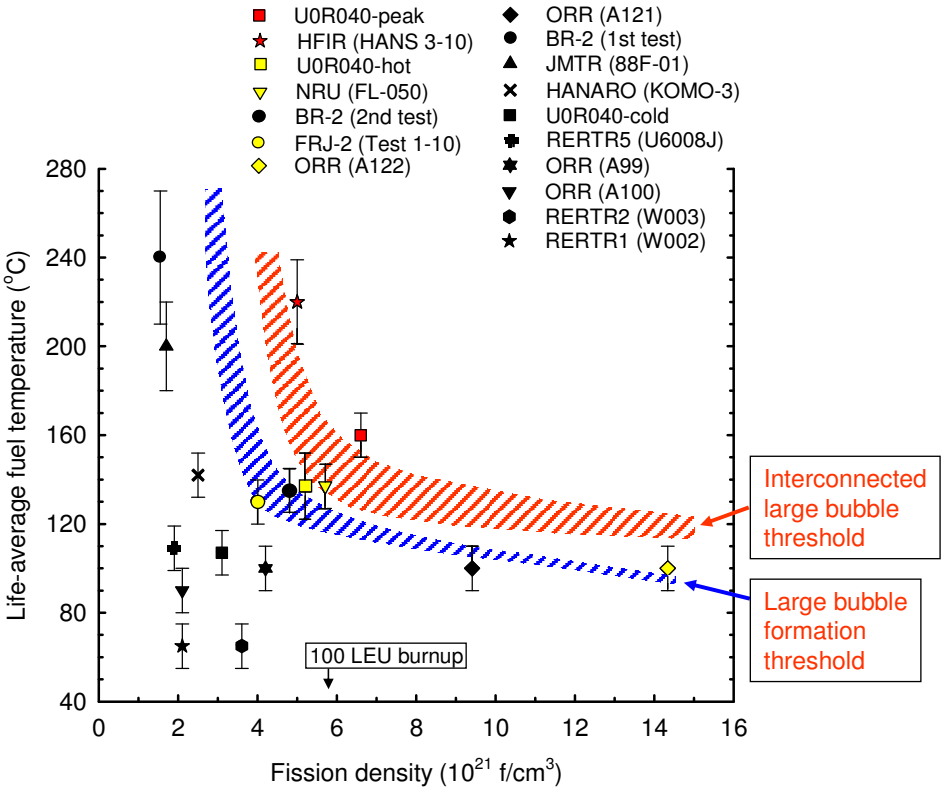

Fig. 3. Fission density-temperature threshold for large bubble formation (greater than 5 μm) and threshold for interconnected gas bubble formation in U_3Si_2. The shaded areas indicate the uncertainty in the thresholds.

After studying all of the available data, a bubble size of 5-μm diameter appears to be a reasonable threshold for characterizing bubbles as being "large." Samples containing large bubbles are designated by colored symbols. Previous observations have shown that bubbles were smaller than ~1 μm for most tests at low temperatures (<110°C). The data shown by red symbols are for those with interconnected bubbles. A combination of sufficiently high fuel temperature and sufficiently high fission density (FD) appears to be necessary for the formation of large bubbles, some of which can become interconnected. Two tentative threshold curves are shown in the figure: one for large bubble formation and the other for interconnected large bubble formation. The FD asymptotically decreases to a threshold value as the temperature increases because a minimum FD is required before large fission gas bubbles can form. On the other hand, the threshold temperature gradually decreases as the FD increases.

The thresholds are shown as shaded areas, indicating considerable uncertainty owing to the sparseness of the dataset. For example, the test results from second BR-2 test and the FRJ-2 test

are on the threshold for large bubble formation. The FRJ-2 test plate contained 6-μm bubbles uniformly distributed in the fuel particles, and the BR-2 test plate contained 3-μm bubbles, although the former has a lower FD than the latter.* Bubble growth is faster in U_3Si than in U_3Si_2. For most of the test samples, however, the local phase inhomogeneity in the fuel particles where the micrographs were taken is unknown. Therefore, it is uncertain whether the large bubbles are indeed included in U_3Si_2.

Therefore, one of the most important variables in the performance of U_3Si_2 is the existence of the so-called secondary phases, viz., U solid solution, U_3Si, or USi. These phases have different gas bubble swelling and interaction layer growth kinetics than U_3Si_2. In general, as the Si/U ratio increases, both bubble growth and IL growth rates decrease. However, it is essentially impossible to produce pure U_3Si_2 at the exact stoichiometric composition. The practice at ANL has been to make slightly Si-rich alloys that lead to final products containing the secondary phases with the maximum amounts of 3 vol% of U solid solution, 10 vol% of U_3Si, or 15 vol% of USi [11]. The secondary phases typically reside inhomogeneously in a fuel particle so that the size of fission gas bubbles varies within a fuel particle, as well as from particle to particle. The postirradiation microstructure of U0R040 also shows this inhomogeneity.

As FD increases, the Si/U ratio of the fuel increases. The question is whether the fuel becomes more stable and, therefore, experiences even slower bubble growth. Comparison of the A-121 and A-122 data in Fig. 3 rejects this possibility. A-122, with a higher FD than A-121, showed large bubble growth while A-121 did not. A possible explanation can be found in the fission product yield. The transition metal elements and rare earth elements are produced at a rate of ~1.3 atoms per fission. Therefore, the increase in the concentrations of fission products is larger than the decrease in the U concentration. Some of the fission products, for example Zr, have higher affinity for Si than U, and form compounds with Si, ultimately reducing the effective Si/U ratio.

A temperature effect can be seen if a comparison is made between the behaviors of W003 from ATR, A-99 from ORR, and Plate #10 from FRJ-2 (see Table 1). These test samples have similar FDs, having been irradiated for long times, but the fuel meat temperatures were different. However, only the FRJ-2 sample, which had the highest temperature of the three samples, contains much larger bubbles than the others. Except for the extremely high FD test of A-122 in ORR, larger than 5-μm bubbles were observed only at fuel meat temperatures higher than 130°C. This phenomenon cannot be explained by the existing athermal swelling model.

Figure 4 is a micrograph showing bubble morphology of U_3Si irradiated at 100°C to a FD of 5.3×10^{21} f/cm^3 in ORR. The bubble morphology is indistinguishable from that of high-temperature U0R040 shown in Fig. 2(c). This shows that bubble growth in U_3Si_2 can be enhanced to the level of U_3Si if the temperature is increased. U_3Si_2 appears to experience a bubble growth phenomenon at high temperatures similar to that of U_3Si at low temperatures—the low bubble growth advantage of U_3Si_2 provided by the high Si/U ratio is negated by increasing the temperature. A theoretical explanation of the temperature effect is given in Sect. 5.

* The BR-2 test plate also contained maximum 21-μm-size bubbles in localized U_3Si phases within the U_3Si_2 fuel particles [2].

It is interesting to compare the U_3Si_2 fuel swelling data obtained from U0R040 with that of U-Mo. Here fuel swelling means the total of gas bubble swelling and solid fission product swelling.

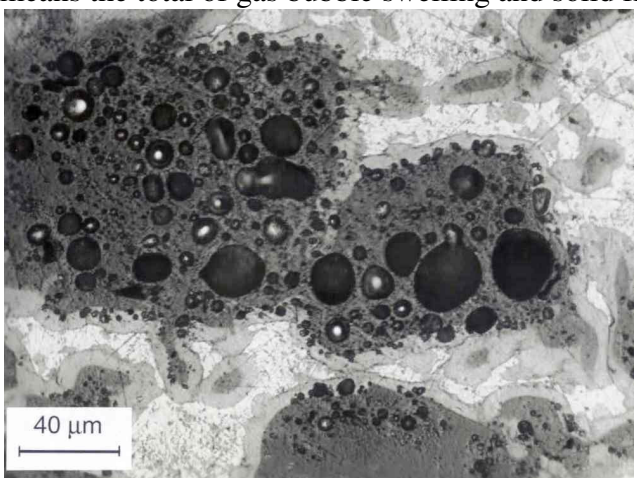

Fig. 4. Optical micrograph of U_3Si-Al irradiated for 319 days to fission density of 5.3×10^{21} f/cm^3 at life-average temperature of 100°C in ORR (A105 plate).

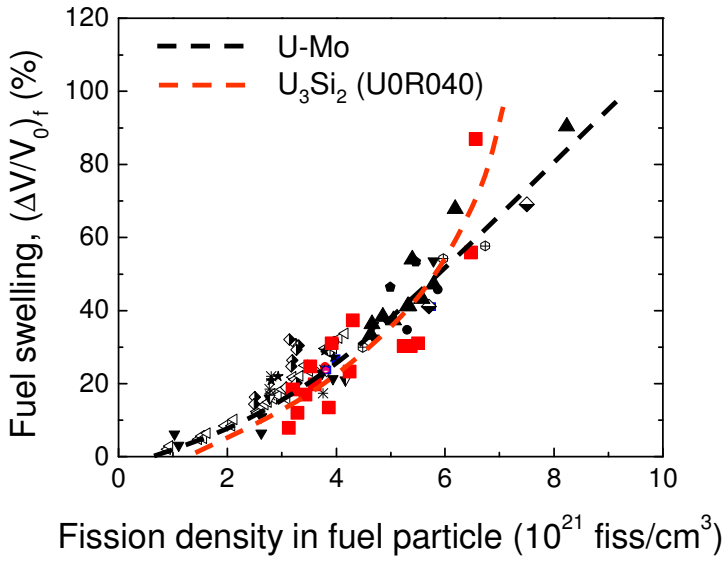

Fig. 5. Comparison of fuel swelling data between U-Mo and U_3Si_2.

Figure 5 shows the comparison after the silicide fuel swelling was adjusted for the as-fabricated fuel meat porosity (10%) that accommodates fuel swelling at low FDs. The fuel temperature of U0R040 is similar to those of the U-Mo plates because the power of U0R040 was similar to the U-Mo test plates, which is higher than typical silicide tests. Particularly U0R040 (irradiated at C-6 position) and H1P010 (irradiated at C-4 position) have similar temperatures because they were so designed and tested in similar test position in the test capsule. As is shown in Fig. 5, fuel swelling of U_3Si_2 is lower than that for U-Mo at low FDs, which is consistent with data

previously available in the literature [12]. However, fuel swelling appears to increase faster for U_3Si_2 than for U-Mo at high FDs as the as-fabrication porosity disappears. This U_3Si_2 swelling rate is also greater than the 6.2% per 10^{21} f/cm^3 measured previously[11]. The high fission density U-Mo data, marked with upward triangles, were obtained from H1P010, irradiated in a neighboring position (C-4) in the same test capsule that included U0R040. The rapid increase in U_3Si_2 fuel swelling at a FD of about 6.5×10^{21} f/cm^3 is due to formation of large bubbles, which ultimately results in higher fuel swelling than U-Mo at the same FD. Because of its lower uranium density, U_3Si_2 has ~30% lower FD at the same burnup as U-10Mo.

The Boosted Fast Flux Loop test, currently under irradiation in the ATR, will provide irradiation data for U_3Si_2 at higher temperatures and, perhaps, FDs than U0R040. When these data become available in the future, the current analysis can be extended.

5. Theoretical interpretation

The extreme behavior shown in Fig. 4 for U_3Si was not observed in the lower density compound U_3Si_2 irradiated at 106°C, where a distribution of relatively small and stable fission gas bubbles was observed to form and remain throughout the irradiation to very high burnup, as shown in Fig. 2(a) [12]. The bubble coarsening process in irradiated amorphous materials such as U_3Si and U_3Si_2 was explained in terms of the material's viscosity [13,14]. The irradiation-induced change in viscosity of a U-Si compound is a strong function of the material's composition. Thus, in order to utilize such models in a quantitative fashion (e.g., to calculate gas-bubble driven swelling), a quantitative estimate of the material's viscosity as a function of composition and irradiation conditions is required.

For the case of irradiation-induced amorphization, the Adam-Gibbs relation [15] for the intrinsic viscosity η is expressed as

$$\eta = \eta_0 \exp\left[\frac{A}{S_c T}\right], \tag{2}$$

where S_c is the configurational entropy, η_0 and A are constants, and T is the absolute temperature.

In order to determine S_c in Eq. (2), the entropy of mixing of solid alloys is calculated using a generalized hard sphere model of binary fluids applied to alloys that undergo an irradiation-induced crystalline-amorphous transformation [16].

Work on ion-beam induced plastic deformation of amorphous solids has revealed that for these conditions the viscosity is inversely proportional to the strain rate [17,18]. Here, the irradiation-induced viscosity η_I is assumed to have a similar dependence on fission rate as it has on strain rate, i.e. the viscosity is inversely proportional to the fission rate $\dot{f}$,

$$\eta_I = \eta \, \dot{f}_0 / \dot{f}\,, \tag{3}$$

where, in general, η is given by Eq. (2), and $\dot{f}_0$ is the minimum fission rate for which the material will remain amorphous.

As shown in Fig. 6, the generalized hard sphere model was used to calculate the viscosity of U-Si as a function of Si/U ratio for three values of the irradiation temperature. The calculated temperature dependence of the viscosity is dependent on an assumption made in the analysis that the rate of change of the calculated formation enthalpy with respect to temperature is symmetric about the uranium concentration corresponding to the curve minimum. In addition, the temperature independence of certain materials properties (such as thermal expansion coefficient) has also been assumed. Thus, only the trend of the calculations should be considered at this time. It is important to note that as U_3Si_2 is irradiated, the Si/U ratio shifts to the right. In any event, the calculations show that a ~30 K increase in temperature results in a viscosity for U_3Si_2 that is similar to that of U_3Si irradiated at the lower temperature. In addition the calculated viscosity of U_3Si_2 is much more sensitive to temperature than that of U_3Si.

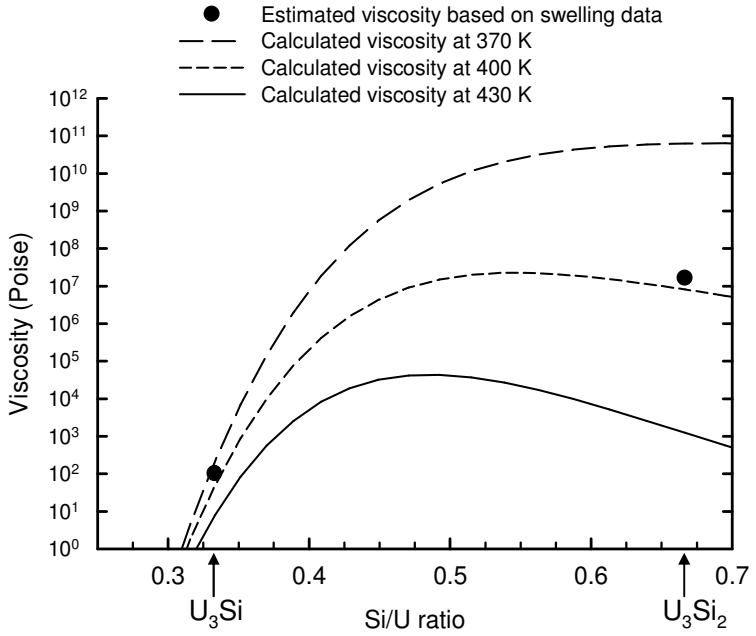

Fig. 6. Viscosity versus Si/U ratio for three temperatures.

6. Conclusion

U0R040 (a U_3Si_2 plate) irradiated as part of the RERTR-8 test was examined. U_3Si_2 showed abnormally large fission gas bubbles. A maximum bubble size of ~40 μm was observed at a fuel life-average temperature of 160°C and a fission density of 6.5×10^{21} f/cm^3. The bubble morphology is similar to that of U_3Si irradiated at low-temperature (<110°C). The existing athermal fuel swelling model appears to be applicable only at low temperatures (T<110°C). At high temperature (130°C<T), the thermal contribution to U_3Si_2 gas bubble growth is considerable.

The interconnected large bubble growth yielded fuel swelling of ~90%, which is greater than U-Mo fuel swelling at the same fission density and temperature. Fuel temperature and fission density are identified as two determining factors for large bubble growth and interconnection of large bubbles. A threshold between individual bubble growth and interconnected large bubble growth is proposed in terms of fuel temperature and fission density.

A model developed at ANL was used to interpret the behavior of fission gas in irradiated amorphous materials such as U_3Si_2 and U_3Si, in which the bubble coarsening process depends on the material's viscosity. The model predictions showed that an ~30 K increase in temperature reduces the viscosity of U_3Si_2 to a level that is similar to that of U_3Si irradiated at the lower temperature, which follows the trend of the observed bubble growth in U0R040. The model also predicts that the gas bubble growth of U_3Si_2 is much more sensitive to temperature than that of U_3Si because the former has a more temperature-sensitive viscosity than the latter.

Acknowledgments

The authors are grateful to Dr. J.L. Snelgrove for his careful review of the paper and comments. The authors would like to thank Dr. D.M. Wachs for the RERTR test. PIE work at the MFC-INL is also appreciated.

References

[1] A. Leenaers, S. Van den Berghe, E. Koonen, P. Jacquet, C. Jarousse, B. Guigon, A. Ballagny, L. Sannen, J. Nucl. Mater., 327 (2004) 121.
[2] A. Leenaers, E. Koonen, Y. Parthoens, P. Lemoine, S. Van den Berghe, J. Nucl. Mater., 375 (2008) 243.
[3] G.L. Hofman, Yeon Soo Kim, J.L. Snelgrove, "Evaluation of U_3Si_2-Al dispersion fuel irradiation behavior in support of the booster fuel design of the ATR Gas-Test-Loop," ANL RERTR Annual report, 2005.
[4] M. Ugajin, M. Akabori, A. Itoh, H. Someya, T. Nakagawa, K. Ohsawa, RERTR Meeting, 1992.
[5] G.L. Hofman, J. Rest, J.L. Snelgrove, T. Wiencek, S. Koster van Groos, RERTR Meeting, 1996.
[6] G.S. Chang, M.A. Lillo, "RERTR as-run physics analysis and test train isotopes, EDF-7868, INL internal report," rev.11, 2006.
[7] Yeon Soo Kim, G.L. Hofman, "Interaction layer growth in U_3Si/Al, U_3Si_2/Al and USi/Al dispersion fuels during irradiation," unpublished work, Argonne National Laboratory, 2008.
[8] H.J. Ryu, J.M. Park, C.K. Kim, private communication, KAERI, 2008.
[9] W. Krug, E. Groos, J. Seferiadis, G. Thamm, RERTR conf., ANL/RERTR/TM-13, 1988.
[10] D. Sears, M.F. Primeau, C. Buchanan, D. Rose, RERTR Meeting, 1994.
[11] J.L. Snelgrove, R.F. Domagala, G.L. Hofman, T.C. Wiencek, G.L. Copland, R.W. Hobbs, R.L. Senn, Argonne National Laboratory, Report ANL/RERTR/TM-11, 1987; also contained as Appendix A in Nuclear Regulatory Commission, "Safety Evaluation Report," NUREG-1313, 1988.
[12] M.R. Finlay, G.L. Hofman, J.L. Snelgrove, J. Nucl. Mater., 325 (2004) 118.
[13] G.L Hofman, Yeon Soo Kim, Nucl. Eng. Tech., 37 (2005) 299.
[14] J. Rest, J. Nucl. Mater., 325 (2004) 107.
[15] G. Adam, J.H. Gibbs, J. Chem. Phys., 43 (1965) 139.
[16] J. Rest, Comput. Mater. Sci., in press, 2008.
[17] S. Klaumunzer, Rad. Effect Defects Solid, 110 (1989) 79.

[18] S. S. Klaumunzer, C. Li, S. Loffler, M. Rammensee, G. Schumacher, H. Ch. Neitzer, Rad. Eff. Defects Solids, 108 (1989) 131.